# Paramagnetic $^1$H NMR Spectroscopy of the Cyanide Derivative of Met80Ala-iso-1-cytochrome *c*

**Kara L. Bren,[†] Harry B. Gray,*[,†] Lucia Banci,[‡] Ivano Bertini,*[,‡] and Paola Turano[‡]**

*Contribution from the Arthur Amos Noyes Laboratory, California Institute of Technology, Pasadena, California 91125, and Department of Chemistry, University of Florence, Via G. Capponi 7, 50121 Florence, Italy*

*Received October 13, 1994*[⊗]

**Abstract:** Mutation of the axial methionine residue (Met80) of iso-1-cytochrome *c* to an alanine gives a ligand-binding protein (Ala80cyt *c*) with spectroscopic features similar to those of myoglobin and peroxidases. $^1$H NMR spectroscopy has been utilized to probe the active-site structure of the cyanide derivative of Ala80cyt *c*. The signals of the axial His18 protons have been assigned by using a superWEFT pulse sequence with variable, short recycle delays and $\tau$ values as well as 1D NOE, 2D NOESY, and COSY experiments. The $^1$H NMR signals of the heme substituents also have been assigned; the similarity of the heme methyl shifts to those of wild-type ferricyt $c$–$CN^-$ indicates that the proximal His orientation is unchanged in the mutant. The large hyperfine shift and short $T_1$ of the signal attributable to the Tyr67 hydroxyl proton suggest that this proton is hydrogen-bonded to the ligated cyanide.

## Introduction

The heme group displays great versatility in nature, functioning in proteins as the active site for oxygen storage and transport (myoglobins and hemoglobins),[1] electron transfer (cytochromes *c*),[2] and redox catalysis (peroxidases,[3] cytochrome P-450[4]). Site-directed mutagenesis experiments have shown that the distal His (position E7) in the heme cavity of myoglobin (Mb) plays a key role in stabilizing the Fe–$O_2$ complex by hydrogen-bonding, while disfavoring Fe–CO bonding.[5–7] It also appears that oxyMb can be stabilized by the presence of an aromatic residue in the distal pocket, since the Leu29Phe mutant of sperm whale Mb exhibits an unusually high Fe–$O_2$ binding constant and low autoxidation rate.[7] In addition, it is likely that a B-helix Phe is responsible for the stability of the Fe–$O_2$ unit in elephant Mb, because there is a Gln at the E7 position.[8]

Both distal and proximal residues affect the reactivity of cytochrome *c* peroxidase (C*c*P).[9–16] The distal His is required for the enzyme's rapid reaction with peroxide to form the iron-(V) intermediate species (compound **I**),[9] and a nearby distal residue, Arg48, has been implicated in compound **I** stabilization.[10] The activity of the enzyme is lost when the proximal ligand (His175) is replaced by Gly to give a bisaqua–heme complex; however, some function is restored in the presence of added imidazole.[11] Work on a related mutant of Mb (His93Gly) in which imidazole and other bases occupy the proximal binding site has shown that small changes in ligand orientation can lead to significant changes in heme function.[12]

A ligand-binding mutant of cytochrome *c*, Ala80cyt *c*, has been produced by both semisynthesis of the horse heart protein[17,18] and site-directed mutagenesis of yeast iso-1-cyt *c*.[19] The resulting heme cavity has remarkable properties. In the

[†] California Institute of Technology.

[‡] University of Florence.

[⊗] Abstract published in *Advance ACS Abstracts*, July 15, 1995.

(1) Antonini, E.; Brunori, M. *Hemoglobin and Myoglobin in their Reactions with Ligands*; North Holland Publishing Co.: Amsterdam, 1971.

(2) Moore, G. R.; Pettigrew, G. W. *Cytochrome c; Evolutionary, Structural and Physicochemical Aspects*; Springer-Verlag: Berlin, 1990. Pettigrew, G. W.; Moore, G. R. *Cytochromes c: Biological Aspects*; Springer-Verlag: Berlin, 1987.

(3) Yonetani, T. In *The Enzymes*, Boyer, P. D., Ed.; Academic Press: Orlando, FL, 1976; Vol. 13, pp 345–361.

(4) Ortiz de Montellano, P. R. *Cytochrome P-450: Structure, Mechanism, and Biochemistry*; Plenum Press: New York, 1986.

(5) Springer, B. A.; Egeberg, K. D.; Sligar, S. G.; Rohlfs, R. J.; Mathews, A. J.; Olson, J. S. *J. Biol. Chem.* **1989**, *264*, 3057–3060.

(6) Smerdon, S. J.; Krzywda, S.; Wilkinson, A. J.; Gibson, Q. H.; Blackmore, R. S.; Dezz Ropp, J.; Sligar, S. G. *Biochemistry* **1991**, *30*, 4697–4705. Smerdon, S. J.; Dodson, G. G.; Wilkinson, A. J.; Gibson, Q. H.; Blackmore, R. S.; Carver, T. E.; Olson, J. S. *Biochemistry* **1991**, *30*, 6252–6260. Rohlfs, R. J.; Mathews, A. J.; Carver, T. E.; Olson, J. S.; Springer. B. A.; Egeberg, K. D.; Sligar, S. G. *J. Biol. Chem.* **1990**, *265*, 3168–3176. Carver, T. E.; Olson, J. S.; Egeberg, K. D.; Springer, B. A.; Sligar, S. G.; Carver, T. E.; Rohlfs, R. J.; Olson, J. S. *J. Biol. Chem.* **1990**, *265*, 11788–11795.

(7) Carver, T. E.; Brantley, R. E., Jr.; Singleton, E. W.; Arduini, R. M.; Quillin, M. L.; Phillips, G. N., Jr.; Olson, J. S. *J. Biol. Chem.* **1992**, *267*, 14443–14450.

(8) Vyas, K.; Rajarathnam, K.; Lu, L. P.; Emerson, S. D.; La Mar, G. N.; Krishnamoorthi, R.; Mizukami, H. *J. Biol. Chem.* **1993**, *268*, 14826–14835.

(9) Erman, J. E.; Vitello, L. B.; Miller, M. A.; Shaw, A.; Brown, K. A.; Kraut, J. *Biochemistry* **1993**, *32*, 9798–9806.

(10) Vitello, L. B.; Erman, J. E.; Miller, M. A.; Wang, J.; Kraut, J. *Biochemistry* **1993**, *32*, 9807–9818.

(11) McRee, D. E.; Jensen, G. M.; Fitzgerald, M. M.; Siegel, H. A.; Goodin, D. B. *Proc. Natl. Acad. Sci. U.S.A.* **1994**, *91*, 12847–12851.

(12) Decatur, S. M.; Boxer, S. G. *Biochemistry* **1995**, *34*, 2122–2129. DePillis, G. D.; Decatur, S. M.; Barrick, D.; Boxer, S. G. *J. Am. Chem. Soc.* **1994**, *116*, 6981–6982. Barrick, D. *Biochemistry* **1994**, *33*, 6546–6554.

(13) Vitello, L. B.; Erman, J. E.; Miller, M. A.; Mauro, J. M.; Kraut, J. *Biochemistry* **1992**, *31*, 11524–11535.

(14) Satterlee, J. D.; Erman, J. E.; Mauro, J. M.; Kraut, J. *Biochemistry* **1990**, *29*, 8797–8804.

(15) Ferrer, J. C.; Turano, P.; Banci, L.; Bertini, I.; Morris, E. K.; Smith, K. M.; Smith, M.; Mauk, A. G. *Biochemistry* **1994**, *33*, 7819–7829.

(16) Fitzgerald, M. M.; Churchill, M. J.; McRee, D. E.; Goodin, D. B. *Biochemistry* **1994**, *33*, 3807–3818. Roe, J. A.; Goodin, D. B. *J. Biol. Chem.* **1993**, *268*, 20037–20045. Goodin, D. B.; McRee, D. E. *Biochemsisry* **1993**, *32*, 3313–3324. Adachi, S.; Magano, S.; Ishimori, K.; Watanabe, Y.; Morishima, I.; Egawa, T.; Kitagawa, T.; Makino, R. *Biochemistry* **1993**, *32*, 241–252. Miller, V. P.; DePillis, G. D.; Ferrer, J. C.; Mauk, A. G.; Ortiz de Montellano, P. R. *J. Biol. Chem.* **1992**, *267*, 89366–8942. Goodin, D. B.; Davidson, M. G.; Roe, J. A.; Mauk, A. G.; Smith, M. *Biochemistry* **1991**, *30*, 4953–4962. Sundaramoorthy, M.; Choudhury, K.; Edwards, S. L.; Poulos, T. L. *J. Am. Chem. Soc.* **1991**, *113*, 7755–7757. Sivaraja, M.; Goodin, D. B.; Smith, M.; Hoffman, B. M. *Science* **1989**, *245*, 738–740.

(17) Wallace, C. J. A.; Clark-Lewis, I. *J. Biol. Chem.* **1992**, *267*, 3852–3861.

(18) Bren, K. L.; Gray, H. B. *J. Am. Chem. Soc.* **1993**, *115*, 10382–10383.

(19) Lu, Y.; Casimiro, D. R.; Bren, K. L.; Richards, J. H.; Gray, H. B. *Proc. Natl. Acad. Sci. U.S.A.* **1993**, *90*, 11456–11459.

0002-7863/95/1517-8067$09.00/0 

ferrous state, Ala80cyt *c* forms a dioxygen complex with a higher binding constant and a lower autoxidation rate than myoglobin.[18,19] In ferriAla80cyt *c*, hydroxide serves as an axial ligand at pH 7; the p$K_a$ of the heme-bound water (6.5) is 3 units lower than that of myoglobin but is comparable to the p$K_a$ measured for the heme-bound water in the CcP Asp235Asn mutant.[13,14] Since there is no histidine in the distal pocket of Ala80cyt *c*, it is of interest whether another residue can assume its role in hydrogen-bonding interactions with Fe−$O_2$ and Fe−OH units. A likely candidate is Tyr67, whose hydroxyl proton is hydrogen-bonded to the sulfur atom of Met80 in the native protein.[20]

We are employing NMR spectroscopy to probe ligand−residue interactions in the hydrophobic distal cavity of Ala80cyt *c*; our work is centered on the ferriheme−cyanide derivative, since a heme−cyanide can function as a hydrogen-bond acceptor.[21] The paramagnetism of ferriheme−$CN^-$ causes increased chemical shift dispersion for protons in the heme region,[22,23] and the fast relaxation of protons nearest the iron allows for selective observation of these nuclei, such as the proximal histidine ring protons.[15,24−26] Interpretation of the results has been aided by the extensive NMR characterization of native cyt *c*[22,23,27−37] as well as related work on the cyanide derivatives of metMb and peroxidases.[14,15,22−26,38−40]

In this paper, we report NMR signals attributable to protons of His18, Tyr67, and the heme of Ala80cyt *c*−$CN^-$. Our data suggest that Tyr67 plays a role analogous to that of the distal His in Mb or a peroxidase by hydrogen-bonding with the Fe−$CN^-$ unit.

## Experimental Section

Wild-type cyt *c* [WTcyt *c* is (H39Q)(C102S)cyt *c*] and Ala80cyt *c* [(H39Q)(M80A)(C102S)cyt *c*] from *Saccharomyces cerevisiae* were expressed and purified as previously reported.[19] The $^1$H NMR samples were prepared by dissolving lyophilized protein in 50 mM phosphate buffer at pH 7.0 to give solutions 1−3 mM in protein. The pH of the NMR samples was adjusted by addition of small volumes of concentrated solutions of NaOH or $H_3PO_4$. The pH was measured (uncorrected for the isotope effect) with an Orion Model 720 pH meter and a Microelectrodes, Inc., Model MI-410 microcombination pH probe.

Depending on the line widths of the resonances of the different species, the $^1$H NMR spectra were recorded on a Bruker MSL 200 (200 MHz) or an AMX 600 (600 MHz) spectrometer. The 200 MHz $^1$H NMR spectra were recorded by using a superWEFT (water-eliminated Fourier transform)[41] pulse sequence with a recycle delay of 200−250 ms. The 600 MHz $^1$H NMR spectra were obtained by using presaturation during the relaxation delay to eliminate the water signal. The two nonexchangeable protons of the proximal histidine ring in the cyanide adducts were identified at 200 MHz by employing a superWEFT pulse sequence with a recycle delay of 10 ms and a $\tau$ value of 10 ms.

Nonselective $T_1$ measurements were taken at 200 MHz with the inversion recovery pulse sequence[42] with delay times between subsequent pulses from 2048 to 0.5 ms and a recycle delay of 2048 ms. The time dependence of the measured intensities of the hyperfine-coupled signals could be fitted to a single exponential. The recovery of magnetization after a nonselective excitation is expected to be essentially exponential in the case of large paramagnetic contributions (with respect to cross relaxation) as is observed in the present case.[43]

The $^1$H nuclear Overhauser effect (NOE) experiments (at 200 and 600 MHz) were performed by using the superWEFT pulse sequence for water signal suppression and were collected as previously reported.[44] Difference spectra were collected by applying the decoupler frequency on- and off-resonance, alternatively, according to the scheme $\omega$, $\omega + \delta$, $\omega$, $\omega - \delta$, where $\omega$ is the frequency of the irradiated signal and $\delta$ is the offset for the off-resonance irradiation. The application of the off-resonance decoupling symmetrically on both sides of the saturated

(20) Takano, T.; Dickerson, R. E. *J. Mol. Biol.* **1981**, *153*, 95−115.
(21) Travaglini Allocatelli, C.; Cutruzzolà, F.; Brancaccio, A.; Brunori, M.; Qin, J.; La Mar, G. N. *Biochemistry* **1993**, *32*, 6041−6049. Qin, J.; La Mar, G. N.; Ascoli, F.; Bolognesi, M.; Brunori, M. *J. Mol. Biol.* **1992**, *224*, 891−897. Lecomte, J. T. J.; La Mar, G. *J. Am. Chem. Soc.* **1987**, *109*, 7219−7220.
(22) Bertini, I.; Turano, P.; Vila, A. J. *Chem. Rev.* **1993**, *93*, 2833−2932 and references therein.
(23) Bertini, I.; Luchinat, C. *NMR of Paramagnetic Molecules in Biological Systems*; Benjamin/Cummings: Menlo Park, CA, 1986.
(24) Banci, L.; Bertini, I.; Pease, E. A.; Tien, M.; Turano, P. *Biochemistry* **1992**, *31*, 10009−10017.
(25) Banci, L.; Bertini, I.; Turano, P.; Tien, M.; Kirk, T. K. *Proc. Natl. Acad. Sci. U.S.A.* **1991**, *88*, 6956−6960.
(26) Banci, L.; Bertini, I.; Turano, P.; Ferrer, J. C.; Mauk, A. G. *Inorg. Chem.* **1991**, *30*, 4510−4516.
(27) Satterlee, J. D. *Annu. Rep. NMR Spectrosc.* **1986**, *17*, 79−178.
(28) Satterlee, J. D.; Moench, S. *Biophys. J.* **1987**, *52*, 101−107. Yi, Q.; Erman, J. E.; Satterlee, J. D. *Biochemistry* **1994**, *33*, 12032−12041.
(29) Redfield, A. G.; Gupta, R. K. *Cold Spring Harbor Symp. Quant. Biol.* **1971**, *36*, 405−411. Gupta, R. K.; Koenig, S. H.; Redfield, A. G. *J. Magn. Reson.* **1972**, *7*, 66−73.
(30) Wüthrich, K. *Proc. Natl. Acad. Sci. U.S.A.* **1969**, *63*, 1071−1078.
(31) Moore, G. R.; Williams, G. *Biochim. Biophys. Acta* **1984**, *788*, 147−150.
(32) Gao, Y.; Lee, A. J. D.; Williams, R. J. P.; Williams, G. *Eur. J. Biochem.* **1989**, *182*, 57−65. Williams, G.; Moore, G. R.; Porteous, R.; Robinson, M. N.; Soffe, N.; Williams, R. J. P. *J. Mol. Biol.* **1985**, *183*, 409−428. Moore, G. R.; Williams. R. J. P. *Eur. J. Biochem.* **1980**, *103*, 493−502. Moore, G. R.; Williams, R. J. P. *Eur. J. Biochem.* **1980**, *103*, 503−512.
(33) Gao, Y.; McLendon, G.; Pielak, G. J.; Williams, R. J. P. *Eur. J. Biochem.* **1992**, *204*, 337−352. Gao, Y.; Boyd, J.; Pielak, G. J.; Williams, R. J. P. *Biochemistry* **1991**, *30*, 1928−1934. Gao, Y.; Boyd, J.; Williams, R. J. P.; Pielak, G. J. *Biochemistry* **1990**, *29*, 6994−7003. Pielak, G. J.; Boyd, J.; Moore, G. R.; Williams, R. J. P. *Eur. J. Biochem.* **1988**, *177*, 167−177. Pielak, G. J.; Atkinson, R. A.; Boyd, J.; Williams, R. J. P. *Eur. J. Biochem.* **1988**, *177*, 179−185.
(34) Thurgood, A. G. P.; Davies, A. M.; Greenwood, C.; Mauk, A. G.; Smith, M.; Guillemette, J. G.; Moore, G. R. *Eur. J. Biochem.* **1991**, *202*, 339−347.
(35) Santos, H.; Turner, D. L. *FEBS Lett.* **1987**, *226*, 179−185. Santos, H.; Turner, D. L. *Eur. J. Biochem.* **1992**, *206*, 721−728.
(36) Feng, Y. Q.; Roder, H.; Englander, S. W. *Biochemistry* **1990**, 29, 3494−3504.
(37) Qi, X. P.; Di Stefano, D. L.; Wand, A. J.; *Biochemistry* **1994**, *33*, 6408−6417. Feng, Y. Q.; Roder, H.; Englander, S. W. *Biophys. J.* **1990**, *57*, 15−22. Wand, A. J.; Di Stefano, D. L.; Feng, Y.; Roder, H.; Englander, S. W. *Biochemistry* **1989**, *28*, 186−194. Feng, Y.; Roder, H.; Englander, S. W.; Wand, A. J.; Di Stefano, D. L. *Biochemistry* **1989**, *28*, 195−203. Wand, A. J.; Englander, S. W. *Biochemistry* **1985**, *24*. 5290−5294.
(38) Banci, L.; Bertini, I.; Kuan, I-C.; Tien, M.; Turano, P.; Vila, A. J. *Biochemistry* **1993**, *32*, 13483−13489.
(39) (a) Rajarathnam, K.; La Mar, G. N.; Chiu, M. L.; Sligar, S. G. *J. Am. Chem. Soc.* **1992**, *114*, 9048−9058. (b) de Ropp, J. S.; La Mar, G. N.; Wariishi, H.; Gold, M. H. *J. Biol. Chem.* **1991**, *266*, 15001−15008. (c) de Ropp, J. S.; Yu, L. P.; La Mar, G. N. *J. Biomol. NMR* **1991**, *1*, 175−190. (d) de Ropp, J. S.; La Mar, G. N. *J. Am. Chem. Soc.* **1991**, *113*, 4348−4340. (e) Thanabal, V.; La Mar, G. N. *Biochemistry* **1989**, *28*, 7038−7044. (f) Emerson, S. D.; Lecomte, J. T. J.; La Mar, G. N. *J. Am. Chem. Soc.* **1988**, *110*, 4176−4182. (g) Thanabal, V.; de Ropp, J. S.; La Mar, G. N. *J. Am. Chem. Soc.* **1988**, *110*, 3027−3035. (h) Thanabal, V.; de Ropp, J. S.; La Mar, G. N. *J. Am. Chem. Soc.* **1987**, *109*, 265−272. (i) Thanabal, V.; de Ropp, J. S.; La Mar, G. N. *J. Am. Chem. Soc.* **1987**, *109*, 7516−7525. (j) Lecomte, J. T. J.; La Mar, G. N. *Eur. Biophys. J.* **1986**, *13*, 373−381. (k) de Ropp, J. S.; La Mar, G. N.; Smith, K. M.; Langry, K. C. *J. Am. Chem. Soc.* **1984**, *106*, 4438−4444. (l) La Mar, G. N.; Davis, N. L.; Parish, D. W.; Smith, K. M. *J. Mol. Biol.* **1983**, *168*, 887−896. (m) La Mar, G. N.; de Ropp, J. S.; Chacko, V. P.; Satterlee, J. D. *Biochim. Biophys. Acta* **1982**, *708*, 317−325.
(40) Satterlee, J. D.; Erman, J. E. *Biochemistry* **1991**, *30*, 4398−4405. Satterlee, J. D.; Erman, J. E.; de Ropp, J. S. *J. Biol. Chem.* **1987**, *262*, 11578−11583. Satterlee, J. D.; Erman, J. E.; La Mar, G. N.; Smith, K. M.; Langry, K. C. *J. Am. Chem. Soc.* **1983**, *105*, 2099−2104. Satterlee, J. D.; Erman, J. E. *J. Biol. Chem.* **1983**, *258*, 1050−1056.
(41) Inubushi, T.; Becker, E. D. *J. Magn. Reson.* **1983**, *51*, 128−133.
(42) Vold, R. L.; Waugh, J. S.; Klein, M. P.; Phelps, D. E. *J. Chem. Phys.* **1986**, *48*, 3831−3832.
(43) La Mar, G. N.; de Ropp, J. S. In *Biological Magnetic Resonance*; Berliner, L. J., Reuben, J., Eds.; Plenum Press: New York, 1993; Vol. 12, pp. 1−78. Banci, L.; In *Biological Magnetic Resonance*; Berliner, L. J., Reuben, J. Eds; Plenum Press: New York, 1993; Vol. 12, pp 79-111. Banci, L.; Bertini, I.; Luchinat, C. *Nuclear and Electron Relaxation. The Magnetic Nucleus-Unpaired Electron Coupling in Solution*; VCH: Weinheim, 1991.
(44) Banci, L.; Bertini, I.; Luchinat, C.; Piccioli, M.; Scozzafava, A.; Turano, P. *Inorg. Chem.* **1989**, *28*, 4650−4656. Unger, S. W.; Lecomte, J. T. J.; La Mar, G. N. *J. Magn. Reson.* **1985**, *64*, 521−526.

signal minimizes the off-resonance effect of the saturation. The phase of the receiver was alternated accordingly, so that a difference free induction decay was directly collected.

TPPI NOESY[45] spectra were recorded with presaturation of the solvent signal during both the relaxation delay and the mixing time. To optimize the detection of cross peaks involving fast-relaxing resonances, NOESY maps at 295 and 303 K in $D_2O$ solution (90% $D_2O$/10% $H_2O$) were recorded on the full spectral width (59.5 ppm) with a recycle time of 550 ms and a mixing time of 15 ms. To optimize the detection of connectivities in the diamagnetic region, NOESY maps in $D_2O$ and $H_2O$ (90% $H_2O$/10% $D_2O$) were recorded on a smaller spectral width (30 ppm) with a recycle time of 800 ms and mixing times of 25 and 100 ms. Analogously, TPPI TOCSY[46] experiments with presaturation during the relaxation delay were recorded on a spectral width of 59.5 ppm (recycle time of 550 ms, spin lock time of 18 ms) and 30 ppm (recycle time of 800 ms and spin lock times of 30, 60, and 90 ms). A COSY[47] map was recorded in $H_2O$ solution on a 30 ppm spectral width (recycle time of 800 ms). A NOE–NOESY[48] experiment with a mixing time of 70 ms was performed by using the conventional NOESY sequence preceded by (180° pulse)–($\tau$ delay) to select relatively fast-relaxing resonances. During the $\tau$ delay (200 ms) the 5-$CH_3$ signal was irradiated selectively. Analogous to the 1D NOE experiments described above, a difference map was obtained by applying the decoupler frequency on- and off-resonance, alternatively, during the $\tau$ delay. The phase of the receiver was alternated accordingly, so that difference free induction decays were collected directly. For all the 2D maps, 1024 experiments were collected with 4096 data points in the F2 direction. The data were multiplied in both dimensions by a pure cosine-squared (NOESY, TOCSY, and NOE–NOESY) and a pure sine-squared (COSY) bell window function and Fourier-transformed to obtain 2048 × 2048 real data points.

The EPR spectra of the cyanide adducts of WTcyt *c* and Ala80cyt *c* (100 mM phosphate buffer, pH 7) were measured at 6 K with a Bruker ER200 spectrometer operating at 9.6 GHz.

## Results

The assignment of hyperfine-shifted signals is an important step in the structural characterization of the heme and axial iron ligands, as well as of the residues surrounding the metal center. The $^1H$ NMR spectrum of ferriAla80cyt *c* indicates a high-spin species below pH 7; the signals that are hyperfine-coupled with the metal ion are dramatically shifted and broadened.[49] As for the analogous Mb and peroxidase systems,[22] the detailed assignment is very difficult, if not impossible, unless specific nuclear labeling is used. The protons of the low-spin species above pH 7 have short nuclear $T_1$ values, similar to those of the high-pH species of metMb, and provide relatively broad resonances. This species also exhibits slow exchange both with the low-pH species and with an additional low-spin species on the high-pH side.[49] However, cyanide binding to ferriAla80cyt *c* induces the formation of a species with particular stability, even at neutral pH, similar to the analogous derivatives of metMb and peroxidases. Cyanide binding gives a species containing a low-spin heme iron with an NMR spectrum characterized by much narrower lines than those seen for both forms of Ala80cyt *c* at neutral pH without bound cyanide.[49] As shown in Figure 1A, two cyanide adducts with an intensity ratio of 10:1 are detected. Since only the heme methyl signals reveal

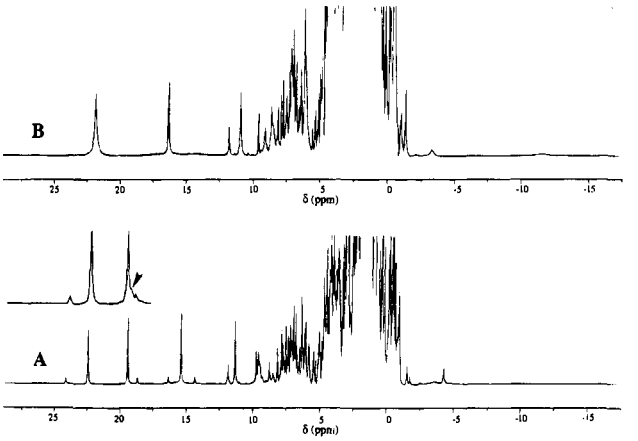


**Figure 1.** $^1H$ NMR (600 MHz) spectra (303 K, 50 mM $NaP_i$, uncorrected pH 7.0, $D_2O$) of (A) Ala80cyt $c-CN^-$ and (B) WTcyt $c-CN^-$. The inset of (A) shows the spectrum recorded in $H_2O$. The arrow indicates the Tyr67 hydroxyl proton resonance.

the existence of two species, they are probably due to different orientations of the heme moiety with respect to the protein matrix, as has been found previously for several heme proteins.[50] For comparison, we also have characterized the cyanide adduct of WTcyt *c*.[30] Cyanide binds to the heme iron in WTcyt *c* and displaces Met80[30,51] to produce a low-spin species characterized by $^1H$ NMR signals (Figure 1B) with a lower shift range with respect to the form without ligated cyanide, but very similar to those of the cyanide adduct of Ala80cyt *c* (Figure 1).

The hyperfine-shifted signals of Ala80cyt $c-CN^-$ have been assigned only for the major species by the combined use of 1D NOE, 2D NOESY, NOE–NOESY, COSY, and TOCSY experiments. To assign the heme substituents, the expected dipolar connectivities based on the WT X-ray crystal structure[52] have been compared to those observed here. This methodology is justified by the fact that CD spectra (not shown) and NMR assignments for the diamagnetic region[53] indicate that the overall fold of Ala80cyt *c* is similar to that of the WT protein.

**Assignment of Heme Substituents.** The four heme methyl signals in the $^1H$ NMR spectrum of Ala80cyt $c-CN^-$ at 303 K are well-resolved at 22.5, 19.5, 15.4, and 11.3 ppm (Figure 1A). The resonances at 22.5 and 15.4 ppm each have a strong dipolar connectivity with a resonance at −4.3 ppm (observed in NOESY maps, Figure 2A, and checked through a 1D NOE experiment, Figure 3). Inspection of the WTcyt *c* X-ray crystal structure[52] reveals that the only proton that can be within NOE distance of two heme methyls is the $\delta$-meso proton that is equidistant from 1-$CH_3$ and 8-$CH_3$. The NOESY map shown in Figure 2A was recorded with a mixing time of 15 ms to enhance the detection of cross peaks between protons with short $T_1$ values. The methyl resonance at 15.4 ppm is dipolarly coupled with $\delta$-$CH_3$ protons of four different Leu residues and with two ring protons of a Phe[53] (data not shown). By inspection of the crystal structure of WTcyt *c*, we assign the methyl signal at 15.4 ppm to 1-$CH_3$, which is close to the side chains of Leu32, Leu68, Leu94, and Leu98 and to the Phe10 ring. The assignment of the resonance

(45) Macura, S.; Wüthrich, K.; Ernst, R. R. *J. Magn. Reson.* **1982**, *47*, 351–357. Marion, D.; Wüthrich, K. *Biochem. Biophys. Res. Commun.* **1983**, *113*, 967–974.
(46) Bax, A.; Davis, D. G. *J. Magn. Reson.* **1985**, *65*, 355–360. Griesinger, C.; Otting, G.; Wüthrich, K.; Ernst, R. R. *J. Am. Chem. Soc.* **1988**, *110*, 7870–7872.
(47) Bax, A.; Freeman, R.; Morris, G. *J. Magn. Reson.* **1981**, *42*, 164–168. Bax, A.; Freeman, R. *J. Magn. Reson.* **1981**, *44*, 542–561.
(48) Bertini, I.; Dikiy, A.; Luchinat, C.; Piccioli, M.; Tarchi, D. *J. Magn. Reson., Ser. B* **1994**, *103*, 278–283.
(49) Banci, L.; Bertini, I.; Bren, K. L.; Gray, H. B.; Turano, P. *Chem. Biol.* **1995**, *2*, 377–383.
(50) Satterlee, J. D.; Erman, J. E. *J. Am. Chem. Soc.* **1981**, *103*, 199–200. La Mar, G. N.; de Ropp, J. S.; Smith, K. M.; Langry, K. C. *J. Am. Chem. Soc.* **1980**, *102*, 4833–4835. La Mar, G. N.; Overkamp, M.; Sick, H.; Gersonde, K. *Biochemistry* **1978**, *17*, 352–361. Keller, R.; Groudinsky, O.; Wüthrich, K. *Biochim. Biophys. Acta* **1976**, *427*, 497–511.
(51) Dickerson, R. E.; Timkovich, R. Cytochromes c. *The Enzymes*; Academic Press: New York, 1975; Vol. XI, pp 397–547.
(52) Louie, G. V.; Hutcheon, W. L. B.; Brayer, G. D. *J. Mol. Biol.* **1988**, *199*, 295–314. Louie, G. V.; Brayer, G. D. *J. Mol. Biol.* **1990**, *214*, 527–555.
(53) Banci, L.; Bertini, I.; Bren, K. L.; Gray, H. B.; Sompornpisut, P.; Turano, P. *Biochemistry*, in press.

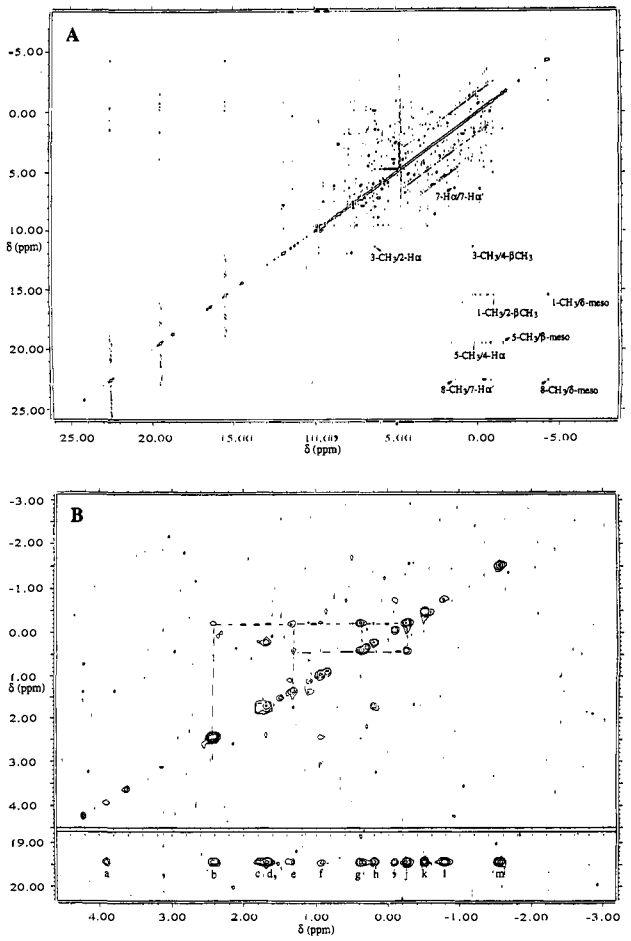


**Figure 2.** (A) $^1$H NMR (600 MHz) TPPI NOESY map of Ala80cyt $c-CN^-$ (303 K, 50 mM $NaP_i$, uncorrected pH 7.0, $D_2O$) recorded over a spectral width of 59.5 ppm using water presaturation during the relaxation delay (550 ms) and the mixing time (15 ms). Resolved cross peaks between heme resonances are labeled. (B) Enlargement of the 600 MHz $^1$H NMR TPPI NOE–NOESY map of Ala80cyt $c-CN^-$ (303 K, 50 mM $NaP_i$, uncorrected pH 7.0, $D_2O$) recorded by using the following pulse sequence: $180°-\tau(200\text{ ms})-90°-t_1-90°-\tau_m(70\text{ ms})-90°-t_2$, with selective saturation of the 5-$CH_3$ resonance during the $\tau$ delay. The signals that are directly coupled with the saturated one lie on the diagonal and at the $\omega_1$ frequency of the saturated signal (inset at bottom). The peaks in the inset are between the 5-$CH_3$ and (a) Gly29 Hα1, (b) Lys79 Hβ, Hβ′, (c) heme 6-Hα, (d) heme 6-Hα′, (e) Lys79 Hδ1, (f) Val28 Hγ2, (g) Lys79 Hε2, (h) heme 6-Hβ, (i) heme 4-Hα, (j) Lys79 Hγ2, (k) Val28 Hγ1, (l) heme β-meso, and (m) Ala80 Hα. Off the diagonal are the cross peaks between the diagonal resonances and other protons close to them. Dotted lines indicate peaks due to the Lys79 residue.

at 22.5 ppm as 8-$CH_3$ is consistent with its NOESY connectivities with Ile, Trp, and Met residues[53] (Ile35, Trp59, and Met64 from the crystal structure of WTcyt *c*).

The two remaining resonances at 19.5 and 11.3 ppm are attributable to the heme methyls 3 and 5. It is possible to distinguish between them on the basis of their dipolar connectivities with other protein residues, expected on the basis of the crystal structure of WTcyt *c*.[52] The resonance at 19.5 ppm is assigned as 5-$CH_3$, since it has NOESY connectivities with a Gly (Gly29) and with some of the side-chain protons of a Lys (Lys79). A NOE–NOESY experiment (Figure 2B) obtained by selective saturation of the resonance at 19.5 ppm was particularly helpful in identifying the connectivities with the Lys79 side chain; several of the protons coupled with the irradiated methyl (Figure 2B, bottom inset) are also coupled with each other. Some of the latter connectivities are also

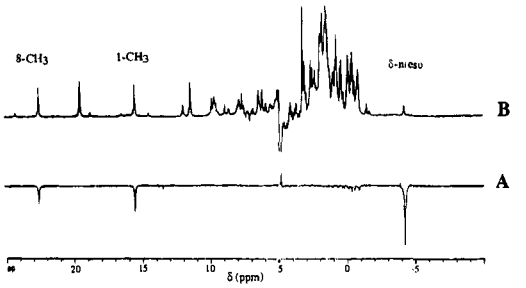


**Figure 3.** (A) 1D NOE difference spectrum of Ala80cyt $c-CN^-$ (303 K, 50 mM $NaP_i$, uncorrected pH 7.0, $D_2O$) recorded by using the superWEFT pulse sequence with a recycle delay of 500 ms and a $\tau$ of 500 ms. (B) $^1$H NMR (600 MHz) reference spectrum. The difference spectrum shows the NOEs observed upon saturation of the δ-meso proton (−4.3 ppm).

**Chart 1.** Schematic Representation of a *c*-Type Heme Showing the Dipolar Connectivities Observed between the Heme Resonances of Ala80cyt $c-CN^-$

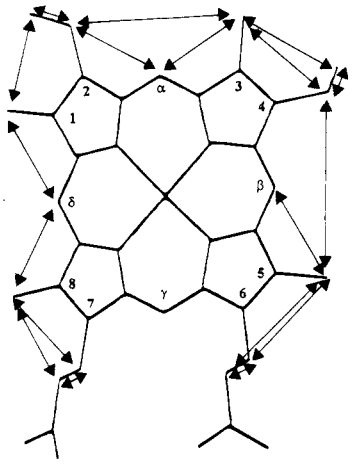


detected in TOCSY experiments, confirming that these signals are due to protons in the same residue, identified as Lys79 by a sequence-specific assignment.[53] The assignment of the resonance at 11.3 ppm to 3-$CH_3$ is confirmed by dipolar connectivities with the ring and β-$CH_2$ protons of a Phe (Phe82).

The remaining heme assignments were made by analyzing NOESY connectivities starting from positions 1 and 3 and continuing around the heme periphery as illustrated in Chart 1. The assignment of the 6-propionate required the use of the aforementioned NOE–NOESY experiment (Figure 2B), which allowed us to identify the propionate chain Hα, Hα′, and Hβ resonances. The 6-Hβ′ resonance remains unassigned. The complete assignment of the 7-propionate was obtained from the NOESY connectivities observed from 8-$CH_3$ to Hα, Hα′, and Hβ′ and those between the 7-propionate resonances (Hα/Hα′, Hα/Hβ, Hα/Hβ′, Hα′/Hβ, Hα′/Hβ′). The Hβ/Hβ′ connectivity is not detectable due to the nearly degenerate shifts (0.6 and 0.8 ppm, respectively) of these two resonances.

A NOESY spectrum of WTcyt $c-CN^-$ recorded at 600 MHz with a mixing time of 15 ms allowed us to assign the heme methyl signals, as reported in Table 1. The NOESY patterns from each of the $CH_3$ resonances are very similar to those observed for Ala80cyt $c-CN^-$ acquired under the same experimental conditions.

**Assignment of Tyr67.** There is a broad exchangeable signal at 19.3 ppm in the spectrum of Ala80cyt *c* in $H_2O$ (inset of Figure 1A). Upon saturation of this signal, NOEs on resonances at 7.8, 7.6, 7.3, and 7.2 ppm are observed. The TOCSY spectrum (Figure 4) shows that these signals belong to a Tyr residue that is not flipping, or is flipping slowly on the NMR

**Table 1.** Assignments for Selected Hyperfine-Shifted Signals in the Spectra of Ala80cyt $c$- and WTcyt $c$-Cyanide Adducts ($T$ = 303 K)

| assignment | Ala80cyt $c$–$CN^-$ signal, ppm | WTcyt $c$–$CN^-$ signal, ppm | assignment | Ala80cyt $c$–$CN^-$ signal, ppm | WTcyt $c$–$CN^-$ signal, ppm |
|---|---|---|---|---|---|
| | | | Heme | | |
| 8-$CH_3$ | 22.5 | 22.2 | 7-H$\alpha'$ | 1.4 | |
| 5-$CH_3$ | 19.5 | 21.8 | 7-H$\beta$ | 0.6 | |
| 1-$CH_3$ | 15.4 | 16.5 | 7-H$\beta'$ | 0.8 | |
| 3-$CH_3$ | 11.3 | 11.1 | 6-H$\alpha$ | 1.8 | |
| 2-H$\alpha$ | 6.3 | | 6-H$\alpha'$ | 1.6 | |
| 2-$CH_3$ | −0.2 | | 6-H$\beta$ | 0.2 | |
| 4-H$\alpha$ | −0.1 | | $\alpha$-meso | 4.1 | |
| 4-$CH_3$ | 0.3 | | $\beta$-meso | −0.8 | |
| 7-H$\alpha$ | 6.3 | | $\delta$-meso | −4.3 | −3.0 |
| | | | His18 | | |
| NHp | 11.0 | 10.6 | H$\delta$1 | 16.6 | 15.0 |
| H$\alpha$ | 9.8 | 9.6 | H$\delta$2 | 16.1 | 22.4 |
| H$\beta$ | 12.0 | 12.0 | H$\epsilon$1 | −3.4 | −11.4 |
| H$\beta'$ | 7.7 | 8.8 | | | |
| | | | Tyr67 | | |
| NHp | 8.8 | | H$\delta$2 | 7.3 | |
| H$\alpha$ | 4.5 | | H$\epsilon$1 | 7.8 | |
| H$\beta$ | 3.3 | | H$\epsilon$2 | 7.6 | |
| H$\beta'$ | 3.5 | | H$\eta$ | 19.3 | 22.2 (288 K) |
| H$\delta$1 | 7.2 | | | | |

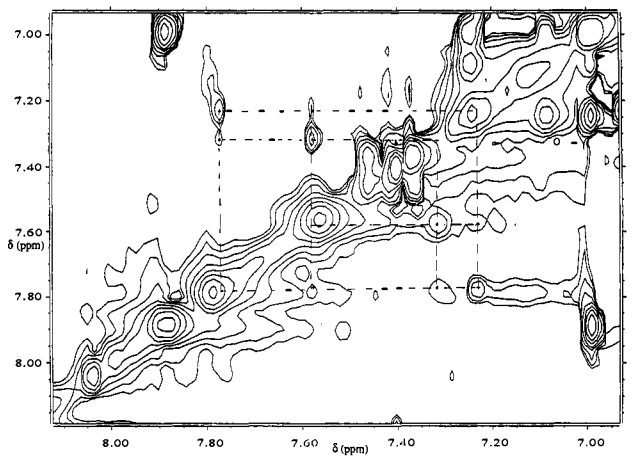


**Figure 4.** $^1H$ NMR (600 MHz) TPPI TOCSY map of Ala80cyt $c$–$CN^-$ (303 K, 50 mM $NaP_i$, uncorrected pH 7.0, $D_2O$) recorded with a spectral width of 30 ppm using water presaturation during the relaxation delay (800 ms) and a spin lock time of 30 ms. Dotted lines define the spin pattern for the Tyr67 ring.

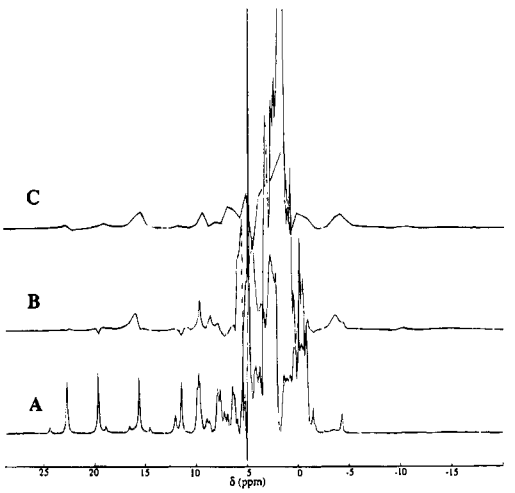


**Figure 5.** $^1H$ NMR (200 MHz) spectra of the cyanide adduct of Ala80cyt $c$ (50 mM $NaP_i$, uncorrected pH 7.0, $D_2O$) recorded by using the superWEFT pulse sequence with different recycle times and $\tau$ values: (A) 250 ms recycle time, 250 ms $\tau$, (B) 33 ms recycle time, 20 ms $\tau$, (C) 10 ms recycle time, 10 ms $\tau$. The broad resonances at 16.1 and −3.4 ppm are due to the H$\delta$2 and H$\epsilon$1 of the proximal His.

time scale. The H$\epsilon$1 of this Tyr gives a NOE with the heme 7-propionate H$\alpha'$. Other NOEs from the above signal at 19.3 ppm are observed on resonances at 6.1, 8.8, and 9.5 ppm, which are the H$\beta$s and H$\gamma$, respectively, of Pro71.[53] No other strong NOEs are detected, thus showing that the above NOEs are not due to spin diffusion. By selectively saturating the heme 5-$CH_3$ resonance, which partially overlaps the resonance at 19.3 ppm, no NOEs are observed on any of the above signals, thus ensuring that they originate from the exchangeable signal. On the basis of these data, this Tyr is identified as Tyr67 and the signal at 19.3 ppm as the exchangeable proton of its ring. Striking features of the 19.3 ppm signal are its large hyperfine shift value and its short $T_1$ value (9 ± 2 ms), which compares with the $T_1$ value of 3 ms for the H$\epsilon$1 proton of His18, which is 3.3 Å from the metal ion.

**Assignment of the Proximal Histidine.** The spectra obtained for Ala80cyt $c$–$CN^-$ by the superWEFT pulse sequence with different repetition times and $\tau$ delays (see Experimental Section) are shown in Figure 5. This procedure[15,24,25] allowed the detection of very broad signals at 16.1 and −3.4 ppm.[54] As reported for the cyanide adducts of peroxidases and Mb, these signals can be attributed to the nonexchangeable ring protons (H$\delta$2 and H$\epsilon$1) of the axial histidine ligand.[22] Saturation of the upfield signal at 200 MHz (because it is sharper than at 600 MHz), as described in the Experimental Section and in previous work,[15,24,25,39e] allows the detection of an NOE with an exchangeable proton that resonates at 16.6 ppm. The presence of this dipolar connectivity is consistent with the assignment of the broad upfield signal as H$\epsilon$1 and the exchangeable signal as H$\delta$1 of the iron-bound histidine (His18). Analysis of the NOESY (Figure 6A) and COSY (Figure 6B) spectra has allowed us to assign all remaining protons of His18 (see Table 1). Specifically, NOESY cross peaks have been detected between H$\delta$1 and three protons of the AMX system of His18, and among the protons of the AMX system. Scalar connectivities defining the His18 AMX spin pattern were observed in TOCSY (data not shown) and COSY (Figure 6B) maps. The signals of the proximal histidine in WTcyt $c$ have

(54) The odd shapes of the signals in Figure 5C are due to the low digital resolution required by the fast recycle time. Zero-filling would provide better shaped resonances. The selective observation of these signals based on different $\tau$ delays is in itself a significant result.

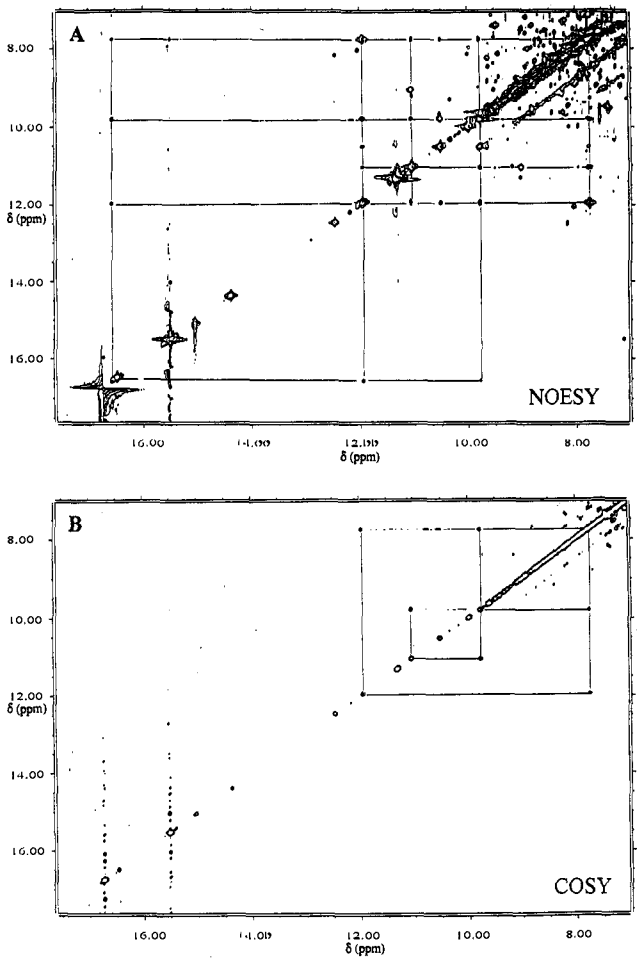


**Figure 6.** Enlargement of 600 MHz $^1$H NMR spectra of Ala80cyt *c* $-CN^-$ (303 K, 50 mM $NaP_i$, pH 7.0) showing the cross peaks between the His18 resonances: (A) TPPI NOESY recorded in $H_2O$ with presaturation of the water signal during the relaxation delay (800 ms) and mixing time (100 ms), (B) magnitude COSY recorded in $D_2O$ with presaturation of the residual water signal during the relaxation delay (800 ms).

been assigned by the same procedure. The shift values are reported in Table 1.

## Discussion

The contact shift is an important contribution to the hyperfine shift for heme methyls in low-spin iron(III) systems.[22,23,55,56] Since the unpaired electron of iron(III) resides in a $d_{xz}$ or $d_{yz}$ orbital, $\pi$ spin density is expected on all heme substituents except for the meso protons, while $\sigma$ spin delocalization should not occur. The heme e($\pi$) orbitals (the HOMOs) that mix with the iron $d_{xz}$ and $d_{yz}$ orbitals have nodes at the meso positions. As a result, the meso protons experience hyperfine shifts that originate predominantly from the pseudocontact term.[55,56] The orientation of the axial ligands strongly influences both the contact and pseudocontact terms, becoming the most important factor in determining the heme methyl and meso proton shift pattern. The interactions of histidine and methionine donor atoms in the axial positions remove the degeneracy of the $d_{xz}$ and $d_{yz}$ orbitals, so that the unpaired electron is only in the upper energy orbital; this gives rise to a characteristic spin-density pattern on the heme.[22,27,56,57] When the *z* axis of the magnetic susceptibility tensor is essentially perpendicular to the heme plane, as is often found for heme proteins,[36,39a,58] the four meso protons all experience the same upfield shift given by the axial term of the pseudocontact contribution. The angular dependence of the rhombic contributions to the pseudocontact term causes alternation between adjacent meso protons.[56] Our experimental data can be rationalized with this picture (Table 1).

The orientation of the axial ligand is important in the definition of the rhombic axes *x* and *y*.[55-59] In Met-ligated hemes, the $sp^3$ lone electron pair on the axial Met sulfur interacts with the $d_{xy}$ and $d_{yz}$ orbitals of the iron. The orientation of the axial Met therefore is believed to determine the *x* and *y* magnetic axes for *c*-type cytochromes.[27,60] Recent data indicate that the histidine orientation also has considerable influence on the asymmetry of the heme electronic structure.[61] The NMR spectrum of WTcyt *c* at pH 7 shows a pairwise pattern for the heme methyl shifts. The two most-shifted methyl resonances (data collected at 303 K) are 8-$CH_3$ (34.6 ppm) and 3-$CH_3$ (31.8 ppm), i.e., the ones on opposite pyrroles. The shift values for the other two heme methyl signals are 10.1 (5-$CH_3$) and 7.1 ppm (1-$CH_3$). The pairwise effect is observed also on the other pyrrole substituents (thioether bridges and propionates). However, analysis of the shift of the protons in position α with respect to the heme, except for the heme methyls, is complicated by the dihedral-angle dependence.[62] We will therefore concentrate on the methyl resonances.

Upon cyanide binding to WTcyt *c*, Met80 is detached from the iron and the heme methyl shift pattern changes completely, being determined only by the orientation of the proximal His ligand. An almost equivalent contact-shift contribution for the four heme methyls is observed, probably due to the orientation of the His ring plane along the α- and γ-meso protons.[59] In this case, the heme methyl resonances have a mean shift value of 17.9 and a spread of only 11.1 ppm, compared to a spread of 27.5 ppm seen for WTcyt *c* without bound cyanide. In the case of metMb$-CN^-$, the histidine plane is oriented along pyrroles 1 and 3 and provides large shifts for methyls 1 and 5. In the case of peroxidases, the proximal His is oriented along pyrroles 2 and 4 (C*c*P)[63a] or along the α- and γ-meso positions (lignin peroxidase).[63b-d] In both cases, large shifts are observed for methyls 3 and 8.

In the spectrum of Ala80cyt *c*$-CN^-$, a mean shift of 17.1 and a spread of 11.2 ppm, similar to the values of WTcyt *c*$-CN^-$, are observed. This indicates that the overall coordination properties, in particular the proximal His orientation,[52] are maintained in the variant. A minor difference in the heme methyl shift pattern is seen for 1-$CH_3$ and 5-$CH_3$, which may be accounted for by assuming small differences in the pseudo-

(55) La Mar, G. N.; Walker, F. A. In *The Porphyrins*; Dolphin, D., Ed.; Academic Press: New York, 1979; pp 61–157.

(56) Lee, K. -B.; La Mar, G. N.; Mansfield, K. E.; Smith, K. M.; Pochapasky, T. C.; Sligar, S. G. *Biochim. Biophys. Acta* **1993**, *1202*, 189–199.

(57) Traylor, T. G.; Berzinis, A. P. *J. Am. Chem. Soc.* **1980**, *102*, 2844–2846. Keller, R. M.; Wüthrich, K. *Biochem. Biophys. Res. Commun.* **1978**, *83*, 1132–1139. La Mar, G. N.; Viscio, D. B.; Smith, K. M.; Caughey, W. S.; Smith, M. L. *J. Am. Chem. Soc.* **1978**, *100*, 8085–8092. Shulman, R. G.; Glarum. S. H.; Karplus, M. *J. Mol. Biol.* **1971**, *57*, 93–115.

(58) Emerson, S. D.; La Mar, G. N. *Biochemistry* **1990**, *29*, 1556–1566.

(59) Walker, F. A.; Benson, M. *J. Phys. Chem.* **1982**, *86*, 3495–3499. Walker, F. A. *J. Am. Chem. Soc.* **1980**, *102*, 3254–3256.

(60) Senn, H.; Böhme, H.; Wüthrich, K. *Biochim. Biophys. Acta* **1984**, *789*, 311–323 and references therein.

(61) Turner, D. L. *Eur. J. Biochem.* **1995**, *227*, 829–837.

(62) Bertini, I.; Turano, P. In *NMR of Paramagnetic Macromolecules*. La Mar, G. N., Ed.; Nato ASI Series; Kluwer Academic: Dordrecht, The Netherlands 1994; see also references therein.

(63) (a) Finzel, B. C.; Poulos, T. L.; Kraut, J. *J. Biol. Chem.* **1984**, *259*, 3027–3036. (b) Edwards, S. L.; Raag, R.; Wariishi, H.; Gold, M. H.; Poulos, T. L. *Proc. Natl. Acad. Sci. U.S.A.* **1993**, *90*, 750–754. (c) Poulos, T. L.; Edwards, S. L.; Wariishi, H.; Gold, M. H. *J. Biol. Chem.* **1993**, *268*, 4429–4440. (d) Pintek, K.; Glumoff, T.; Winterhalter, K. *FEBS Lett.* **1993**, *315*, 119–124.

contact contribution. Consistent with this hypothesis, we observe a slightly different shift for the δ-meso proton of Ala80cyt *c* compared to WTcyt *c* and a more significant difference for the His18 Hε1 and Hδ2 ring protons, which have been shown to be very sensitive to differences in the orientation of the *z* axis of the magnetic susceptibility tensor.[39a,58] The **g** values for WTcyt $c-CN^-$ and Ala80cyt $c-CN^-$ measured at 6 K are $g_z = 3.28$, $g_y = 2.03$, and $g_x = 1.2$ and $g_z = 3.30$, $g_y = 1.99$, and $g_x = 1.2$, respectively. If there is a difference in the pseudocontact shift between the two proteins, this must be due to differences in the orientation of the magnetic susceptibility tensor and not in its magnitude, because the **g** values are virtually the same. The shift values of the Ala80cyt $c-CN^-$ His18 Hε1 and Hδ2 ring protons (−3.4 and 16.1 ppm, respectively) have a pattern similar to those in cyanide derivatives of peroxidases (where the shift of these two ring protons are, respectively, −29.9 and 23.1 for horseradish peroxidase, −20.6 and 15.8 for *Cc*P, −9.0 and 13.3 for lignin peroxidase, −11.8 and 20.3 for manganese peroxidase, and −9.7 and 14.6 for Asp235Ala *Cc*P).[15,24,25,38] A reverse pattern (19.2 and −4.7 ppm for Hε1 and Hδ2) is observed in the spectrum of the cyanide derivative of Mb.[22,39a]

The temperature dependence of the hyperfine shifts is related to the energy separation between the ground and the excited levels, which, in turn, is modulated by interactions between the iron and the axial ligands. For the low-spin neutral form of ferriWTcyt *c*, it has been found that the shifts of methyls 1 and 5 increase with temperature, while methyls 3 and 8 exhibit normal Curie behavior.[64] This anti-Curie effect has been interpreted in terms of a Boltzmann distribution between two partially filled $d_{xz}$- and $d_{yz}$-symmetry molecular orbitals, assuming a splitting of 3 kJ $mol^{-1}$.[65] A similar anti-Curie effect was not observed for the Ala80 and WT cyanide adducts.

In the distal cavity of Ala80cyt $c-CN^-$, the Tyr67 ring hydroxyl proton exhibits a large hyperfine shift value and short $T_1$, indicating that it experiences significant hyperfine coupling with the unpaired electron. Comparison of the $T_1$ value of this signal (9 ± 2 ms) with that of Hε1 of His18 (3 ms, 3.3 Å from the iron) suggests that the Tyr67 hydroxyl proton is 4 ± 0.2 Å from the iron.[66] Since the $T_1$ of the bulk water is ~0.70 s, the system is in the slow exchange limit. Also, because the $T_1$ is nonselective, the effect that any exchange may have on the $T_1$ of the OH signal does not alter the determination of the iron−proton distance beyond the uncertainty given above. The corresponding signal in WTcyt *c* is observed only at lower temperatures (288 K or below), indicating that this proton in WTcyt *c* is exchanging faster than in the mutant.

In cyanide derivatives of metMb and peroxidases, the broad resonance of a proton with similar relaxation properties and slow exchange with bulk water has been assigned to a labile distal His ring proton that is believed to be H-bonded to the cyanide nitrogen.[26,39ej,67] We propose that, in analogy to the metMb and peroxidase systems, the Tyr67 hydroxyl hydrogen bonds to the cyanide nitrogen. This is confirmed by NOEs from the Tyr protons that allow us to locate the residue in the 3D structure.[53] The presence of hydrogen-bonding between the Tyr67 hydroxyl proton and the cyanide nitrogen suggests that a similar interaction may occur between Tyr67 and $O_2$ bound to the reduced mutant, analogous to the hydrogen-bonding involving the distal histidine in the oxy or carbonmonoxy derivative of Mb.[68]

**Acknowledgment.** We thank Yi Lu for helpful discussions. K.L.B. acknowledges a Kodak graduate fellowship. This work was supported by the National Science Foundation (U.S.A.) and the CNR (Italy).

**Supporting Information Available:** Plots showing heme 8-$CH_3$ magnetization recovery after a nonselective $T_1$ experiment and the fit of these data to a single exponential (2 pages). This material is contained in many libraries on microfiche, immediately follows this article in the microfilm version of the journal, can be ordered from the ACS, and can be downloaded from the Internet; see any current masthead page for ordering information and Internet access instructions.

JA943352C

(64) Senn, H.; Wüthrich, K. *Biochim. Biophys. Acta* **1983**, *743*, 69−81.
(65) Turner, D. L. *Eur. J. Biochem.* **1993**, *211*, 563−568.
(66) When nonselective $T_1$ values are lower than 100 ms, the recovery of the magnetization after a nonselective excitation shows exponential behavior which, therefore, can be fitted to a single exponential (see the supporting information). This means that the dominant contribution to nuclear relaxation is the coupling between the resonating nucleus and the unpaired electron, and it is therefore related to the inverse sixth power of the metal−nucleus distance.
(67) Cutnell, J. D.; La Mar, G. N.; Kong, S. B. *J. Am. Chem. Soc.* **1981**, *103*, 3567−3572.
(68) Kuriyan, J.; Wilz, S.; Karplus, M.; Petsko, G. A. *J. Mol. Biol.* **1986**, *192*, 133−154.